New single-carrier transceiver scheme based on the discrete sine transform

Faisal Al-kamali

Department of Electrical, Faculty of Engineering and Architecture, IBB University, IBB, Yemen
E-mail: faisalalkamali@yahoo.com

Published in *The Journal of Engineering*; Received on 7th November 2013; Accepted on 18th April 2014

Abstract: A discrete sine transform (DST)-based single-carrier transceiver scheme for broadband wireless communications is proposed and investigated. The proposed scheme uses a DST rather than the conventional discrete Fourier transform (DFT) as a basis function to implement the single-carrier system. The performance of the proposed scheme is studied and compared with the DFT-based single-carrier transceiver scheme and the discrete cosine transform based single-carrier transceiver scheme. Simulation results for single-carrier frequency division multiple access system are presented to demonstrate the effectiveness of the proposed scheme for broadband wireless communications.

1 Introduction

Wireless digital communication is rapidly expanding, resulting in a demand for wireless systems that are reliable and have a high spectral efficiency. In recent years, the single-carrier transmission technique such as single-carrier frequency division multiple access (SC-FDMA) has gained more and more attention when it comes to proposals for future wireless communication systems [1–4]. The main advantages of SC-FDMA system is the flexibility that arises from the fact that the total bandwidth is subdivided into many different subcarriers and the low peak-to-average power ratio (PAPR) as compared to the multicarrier systems [2]. This fact motivates the manufacturers to introduce this method in the uplink of long-term evolution (LTE), since reducing the sensitivity to non-linear amplification is of special relevance to mobile terminals [1]. There are two subcarrier mapping methods for the SC-FDMA system. The SC-FDMA system with blockwise subcarriers allocation is known as localised frequency division multiple access (LFDMA) [4]. The SC-FDMA system with regularly interleaved subcarriers allocation is also known as interleaved frequency division multiple access (IFDMA) [3].

In the literature, only the discrete Fourier transform (DFT) and the discrete cosine transform (DCT) were proposed to implement the SC-FDMA system [2–6]. The DFT- based SC-FDMA (DFT-SC-FDMA) system with the localised subcarrier mapping scheme has been adopted as the modulation and demodulation scheme of choice in the 3GPP LTE standard. In [5, 6], it was shown that the DCT-based SC-FDMA (DCT-SC-FDMA) system provides better performance than that of the DFT-SC-FDMA system, even in the presence of carrier frequency offset. Moreover, its PAPR is lower than that of the orthogonal frequency division multiple access (OFDMA). Up to now, the DST-based SC-FDMA (DST-SC-FDMA) system is not studied in the literature. DST uses only real arithmetics rather than the complex arithmetics used in the DFT. This reduces the signal processing complexity, and the in-phase/quadrature imbalance.

In this paper, we introduce a new single-carrier transceiver scheme based on the DST. The proposed transceiver uses a DST, rather than the DFT or the DCT, to implement the SC-FDMA system. The proposed scheme is described and its model is derived. Then, the bit error rate (BER) and the PAPR performances of the proposed DST-SC-FDMA scheme are studied and compared with the existing schemes. In contrast to the conventional DFT-SC-FDMA system, it is found that DST-SC-FDMA provides good BER performance and an acceptable PAPR performance, especially with the localised mapping scheme.

The rest of the paper is organised as follows. Section 2 introduces an overview about DST. Section 3 derives the system model of the proposed DST-SC-FDMA system. Section 4 briefly introduces the DFT-SC-FDMA system. Section 5 is about the DCT-SC-FDMA system. The PAPR problem is discussed in Section 6. Experimental results are given in Section 7. Finally, Section 8 concludes the paper.

2 Discrete sine transform (DST)

In mathematics, the DST is a Fourier-related transform similar to the DFT, but using a purely real matrix. It is equivalent to the imaginary parts of a DFT of roughly twice the length, operating on real data with odd symmetry. DSTs are widely employed in solving partial differential equations by spectral methods, where the different variants of the DST correspond to slightly different odd/even boundary conditions at the two ends of the array [7]. There are several types of the DST with slightly modified definitions. In this Letter, DST-I is considered. For simplicity, it is denoted by DST. The DST is given by

$$y(k) = \sum_{n=1}^{N} x(n)\sin\left(\pi\frac{kn}{N+1}\right), \quad k = 1, 2, \ldots, N \tag{1}$$

The inverse DST (IDST) is given by

$$x(n) = \frac{2}{N+1}\sum_{k=1}^{N} y(k)\sin\left(\pi\frac{kn}{N+1}\right), \quad n = 1, 2, \ldots, N \tag{2}$$

3 DST-SC-FDMA system

The complex exponential functions set are not the only orthogonal basis that can be used to construct baseband single-carrier signals. A single set of cosinusoidal and sinusoidal functions can be used as an orthogonal basis to implement the single-carrier scheme [5]. Fig. 1 describes the transceiver block diagram of the DST-SC-FDMA system. At the transmitter, the input data sequence of the uth user is encoded. The coded bits are mapped to multilevel symbols in one of modulation formats such as quadrature phase shift keying (QPSK), and 16-quadrature amplitude modulation (16QAM). The modulated symbols are grouped into blocks, each containing N symbols, followed by an N-point DST. The subcarrier mapping block assigns the DST outputs into M ($\geq N$) subcarriers that can be transmitted, and inserts zeros into any unused subcarriers. After performing an M-point IDST, a cyclic prefix (CP) is appended at the head of IDST outputs.

In matrix notation, the transmitted signal of the uth user (u = 1,2, …, U) can be formulated as follows

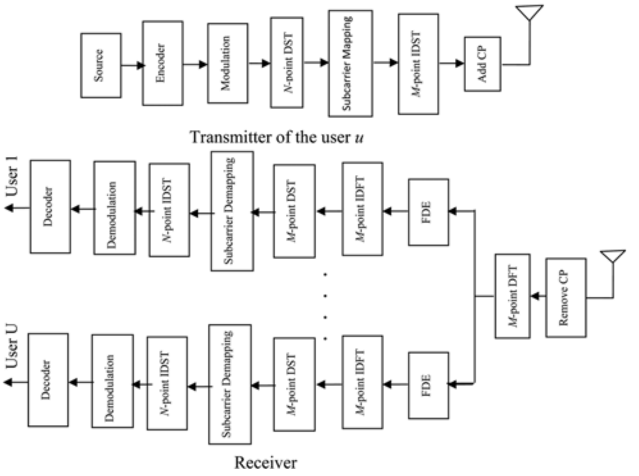

Fig. 1 *Structure of the DST-SC-FDMA system over a frequency selective channel*

$$\tilde{\boldsymbol{x}}_{\boldsymbol{u}} = \boldsymbol{\Pi} \boldsymbol{S}_M^{-1} \boldsymbol{\Gamma}_u \boldsymbol{S}_N \boldsymbol{x}_{\boldsymbol{u}} \quad (3)$$

where $\boldsymbol{x}_u$ is an $N \times 1$ vector containing the modulated symbols of the uth user. $\boldsymbol{S}_N$ is an $N \times N$ DST matrix. $\boldsymbol{S}_M^{-1}$ is an $M \times M$ IDST matrix. $\boldsymbol{\Gamma}_T^u$ is an $M \times N$ matrix describing the subcarriers mapping of the uth user. $M = Q \cdot N$, where Q is the maximum number of users that can transmit, simultaneously. $\boldsymbol{\Pi}$ is an $(M + N_C) \times M$ matrix, which adds a CP of length N_C.

The entries of $\boldsymbol{\Gamma}_u$ for both the localised and the interleaved systems are given in (4) and (5), respectively:

$$\boldsymbol{\Gamma}_u = \left[\boldsymbol{0}_{(u-1)N \times N}; \boldsymbol{I}_N; \boldsymbol{0}_{(M-uN) \times N}\right] \quad (4)$$

$$\boldsymbol{\Gamma}_u = \left[\boldsymbol{0}_{(u-1) \times N}; \boldsymbol{u}_1^{\mathrm{T}}; \boldsymbol{0}_{(Q-u) \times N}; \ \ldots; \boldsymbol{0}_{(u-1) \times N}; \boldsymbol{u}_N^{\mathrm{T}}; \boldsymbol{0}_{(Q-u) \times N}\right] \quad (5)$$

where $\boldsymbol{I}_N$ and $\boldsymbol{0}_{Q' \times N}$ matrices denote the $N \times N$ identity matrix and the $Q' \times N$ all-zero matrix. $\boldsymbol{u}_l$ ($l = 1, 2, \ldots, N$) denotes the unit column vector, of length N, with all zero entries except at l. $\boldsymbol{\Pi}$ can be represented as follows

$$\boldsymbol{\Pi} = [\boldsymbol{C}, \boldsymbol{I}_M]^{\mathrm{T}} \quad (6)$$

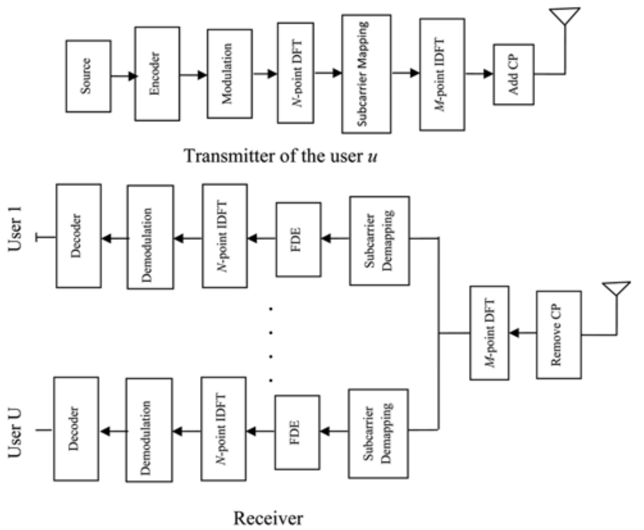

Fig. 2 *Structure of the DFT-SC-FDMA system over a frequency selective channel*

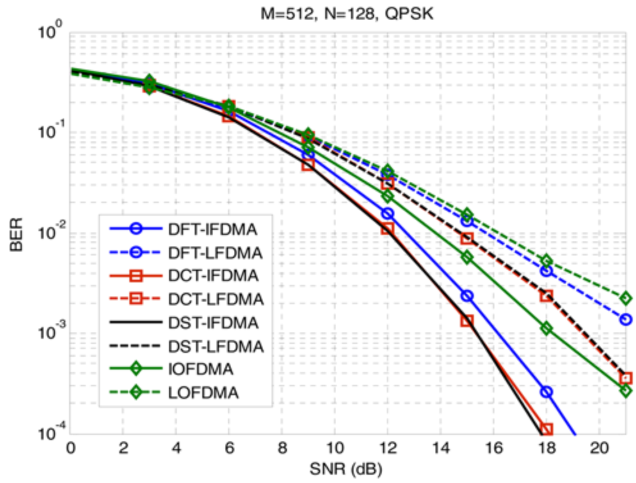

Fig. 3 *BER against the SNR for DFT-SC-FDMA, DCT-SC-FDMA, DST-SC-FDMA and OFDMA systems with different subcarrier mapping schemes and QPSK*

where

$$\boldsymbol{C} = \left[\boldsymbol{0}_{N_C \times (M-N_C)}, \boldsymbol{I}_{N_C}\right]^{\mathrm{T}} \quad (7)$$

At the receiver side, the CP is removed from the received signal and the received signal can be written as follows

$$\boldsymbol{r} = \sum_{u=1}^{U} \boldsymbol{H}_u \bar{\boldsymbol{x}}_u + \boldsymbol{n} \quad (8)$$

where $\bar{\boldsymbol{x}}_u$ is an $M \times 1$ vector representing the block of the transmitted symbols of the uth user. $\boldsymbol{H}_u$ is an $M \times M$ circulant matrix describing the multipath channel between the uth user and the base station. $\boldsymbol{n}$ is an $M \times 1$ vector describing the additive noise. Applying the DFT, we obtain

$$\boldsymbol{R} = \sum_{u=1}^{U} \boldsymbol{\Lambda}_u \boldsymbol{F}_M \bar{\boldsymbol{x}}_u + \boldsymbol{N} \quad (9)$$

where $\boldsymbol{\Lambda}_u$ is an $M \times M$ diagonal matrix containing the DFT of the circulant sequence of $\boldsymbol{H}_u$. $\boldsymbol{N}$ is the DFT of $\boldsymbol{n}$. $\boldsymbol{F}_M$ is an $M \times M$ DFT

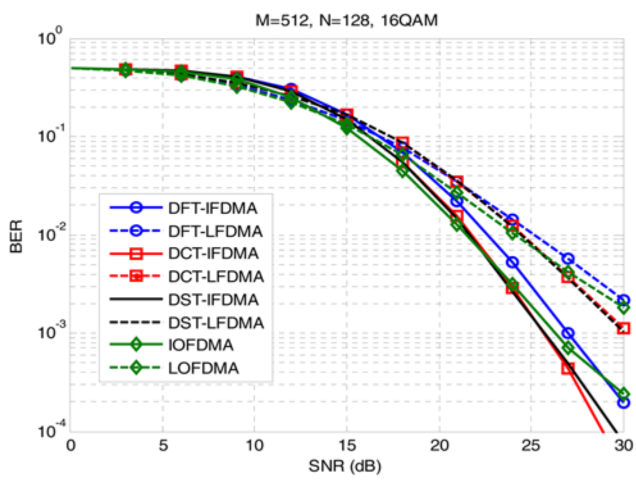

Fig. 4 *BER against the SNR for DFT-SC-FDMA, DCT-SC-FDMA, DST-SC-FDMA and OFDMA systems with different subcarrier mapping schemes and 16QAM*

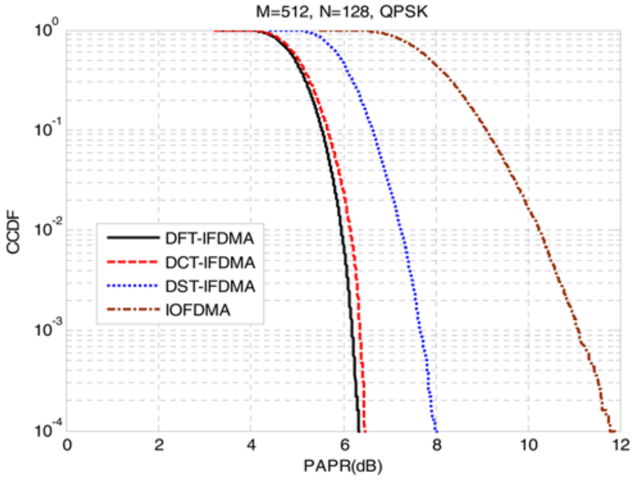

Fig. 5 *CCDFs of the PAPR for DFT-IFDMA, DCT-IFDMA, DST-IFDMA and IOFDMA systems with QPSK*

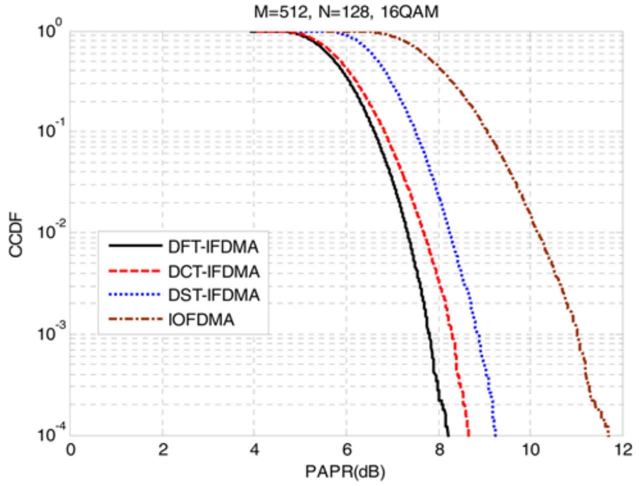

Fig. 7 *CCDFs of the PAPR for DFT-IFDMA, DCT-IFDMA, DST-IFDMA and IOFDMA systems with 16QAM*

matrix. The generic M-point DFT matrix has entries $[\boldsymbol{F}_M]_{p,\ q} = \mathrm{e}^{-\mathrm{j}2\pi(pq/M)}$, and its inverse DFT (IDFT) is $\boldsymbol{F}_M^{-1} = (1/M)\boldsymbol{F}_M^H$.

After that, the FDE, the M-point IDFT and the DST-SC-FDMA demodulation operations are performed to provide the estimate of the modulated symbols as follows

$$\hat{\boldsymbol{x}}_u = \boldsymbol{S}_N^{-1}\boldsymbol{\Gamma}_u^{\mathrm{T}}\boldsymbol{S}_M\boldsymbol{F}_M^{-1}\boldsymbol{W}_u\boldsymbol{R} \tag{10}$$

where $\boldsymbol{W}_u$ is the $M \times M$ FDE matrix of the uth user. Finally, the demodulation and the decoding processes are applied.

4 DFT-SC-FDMA system

A conventional DFT-SC-FDMA transceiver block diagram is shown in Fig. 2. There are U uplink users communicating with a base station through independent multipath fading channels. A total of M subcarriers is assumed and each user is assigned N subcarriers. In the DFT-SC-FDMA transmitter, the encoded signals are modulated and then transformed into the frequency domain via an N-point DFT. Then, the subcarriers are mapped in the frequency domain. After that, IDFT is performed, and a CP is added to the resulting signal. Finally, the resulting signal is transmitted through the wireless channel.

At the receiver, the CP is removed and the DFT is then applied. Finally, the subcarrier demapping, the equalisation, the IDFT, the demodulation and the decoding operations are performed.

5 DCT-SC-FDMA system

The structure of the DCT-SC-FDMA system is similar to that of the DST-SC-FDMA system in Section 3. The difference is that the DST and the IDST blocks at the transmitter and receiver are replaced by the DCT and the IDCT blocks, respectively. More details about the DCT-SC-FDMA system are found in [5].

In this paper, the DFT-based IFDMA is denoted by DFT-IFDMA, the DFT-based LFDMA is denoted by DFT-LFDMA, the DCT-based IFDMA is denoted by DCT-IFDMA, the DCT-based LFDMA is denoted by DCT-LFDMA, the DST-based IFDMA is denoted by DST-IFDMA, the DST-based LFDMA is denoted by DST-LFDMA, the DFT-based interleaved OFDMA is denoted by IOFDMA, and the DFT-based localised OFDMA is denoted by LOFDMA.

6 Peak power problem

The peak power problem causes the non-linear distortion in the power amplifier and reduces power efficiency [8]. The metric used to measure the impact of this problem is the PAPR. PAPR

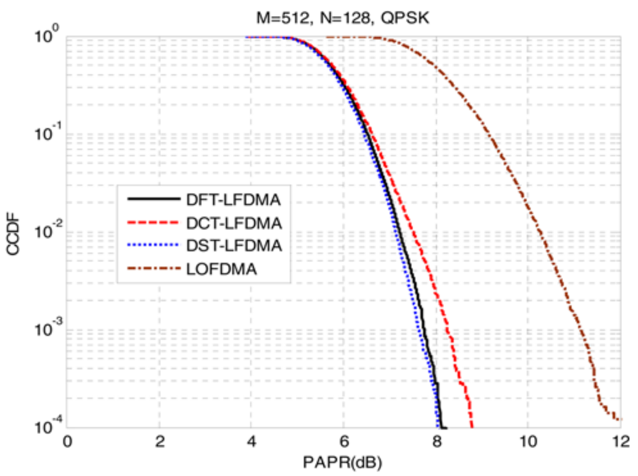

Fig. 6 *CCDFs of the PAPR for DFT-LFDMA, DCT-LFDMA, DST-LFDMA and LOFDMA systems with QPSK*

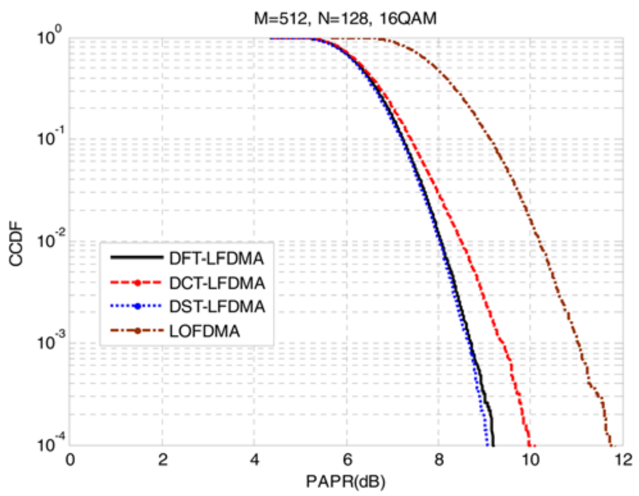

Fig. 8 *CCDFs of the PAPR for DFT-LFDMA, DCT-LFDMA, DST-LFDMA and LOFDMA systems with 16QAM*

Table 1 PAPR values at a CCDF = 10^{-4} for different systems

Modulation format, dB	DFT-IFDMA, dB	DFT-LFDMA, dB	DCT-IFDMA, dB	DCT-LFDMA, dB	DST-IFDMA, dB	DST-LFDMA, dB	IOFDMA and LOFDMA, dB
QPSK	6.5	8	6.6	8.8	8	8	11.75
16-QAM	8.25	9.25	8.75	10	9.25	9.25	11.75

is a commonly used measure of the range of a signal's amplitude. It is a reasonably good qualitative measure; signals with low PAPR generally require less power backoff and exhibit less performance sensitivity when amplified by a non-linear power amplifier than do signals with high PAPR [8]. An informative metric is the complementary cumulative distribution (CCDF) function of the signal amplitude measured over many samples. CCDF is the probability that the PAPR is higher than a certain PAPR value. The PAPR in dB can be expressed as [8]

$$\text{PAPR(dB)} = 10.\log_{10}\left(\frac{\max\left(|x(m)|^2\right)}{(1/M)\sum_{m=0}^{M-1}|x(m)|^2}\right) \tag{11}$$

where $x(m)$ is the mth symbol of the transmitted signal.

7 Simulation results

7.1 Simulation parameters

Monte Carlo simulation is used to evaluate the performance of the proposed DST-SC-FDMA system with different subcarriers mapping methods. For comparison purposes, the DFT-SC-FDMA, the DCT-SC-FDMA and the OFDMA systems are also simulated. In the simulated DST-SC-FDMA system, each user occupies 128 subcarriers. The total number of subcarriers $M = 512$ and the number of users $U = 4$. In each Monte Carlo realisation, all subcarriers are assigned among all users according to the subcarriers mapping method used. QPSK and 16QAM modulation schemes are used to generate a transmitted block for each user. The channel model used for simulations is the vehicular A model [9]. A convolutional code with memory length 7 and octal generator polynomials (133, 171) is chosen as the channel code.

7.2 BER performance

The BER performances for DST-SC-FDMA, DCT-SC-FDMA, DFT-SC-FDMA and OFDMA systems are simulated in Figs. 3 and 4 for the QPSK and the 16QAM, respectively. For each plot, it is clear that the performance of the DST-SC-FDMA system is better than that of the DFT-SC-FDMA and the OFDMA systems, especially with the QPSK. From the figures, it can be seen that the DST-SC-FDMA and the DCT-SC-FDMA systems provide the same performance with both the interleaved and the localised methods. At a BER = 10^{-3} with QPSK, the performance gain is about 2 dB for the DST-LFDMA system, and about 1 dB for the DCT-IFDMA system when compared to that of the DFT-LFDMA system and the DFT-IFDMA system, respectively. This is attributed to the energy concentration property of the DST.

7.3 PAPR performance

Figs. 5 and 6 illustrate the CCDFs of the PAPR for DST-SC-FDMA, DFT-SC-FDMA, DCT-SC-FDMA and OFDMA signals for the case of QPSK and for different subcarrier mapping schemes. Raised cosine pulse shaping filter with roll-off factor = 0.2, and 4 times oversampling is used. From Fig. 5, it is observed that the DST-IFDMA provide considerable gain in PAPR when compared to that of the IOFDMA system. However, it provides high PAPR when compared with that of the DFT-IFDMA and the DCT-IFDMA systems. From Fig. 6, it is shown that the PAPR of the DST-LFDMA signal is comparable to that of the conventional DFT-LFDMA and it is better than that of the DCT-LFDMA and the LOFDMA systems.

Figs. 7 and 8 plot the CCDF of the PAPR for DST-SC-FDMA, DFT-SC-FDMA, DCT-SC-FDMA and OFDMA signals for the case of 16QAM. Raised cosine pulse shaping filter with roll-off factor = 0.2, and 4 times oversampling is used. It is clearly seen that the PAPR of the DST-LFDMA is lower than that of the DCT-LFDMA and the LOFDMA systems. It is also noted that the PAPR of the DST-IFDMA is greater than that of the DFT-IFDMA and the DCT-IFDMA by about 1 and 0.5 dB, respectively.

Since the localised mapping is the subcarriers mapping method of the LTE standard and based on the previous figures, the proposed DST-LFDMA is more suitable for the future wireless communications since it provides better BER performance than that of the conventional DFT-LFDMA system and it has the same PAPR as that of the conventional DFT-LFDMA system.

A full comparison of PAPR at a CCDF = 10^{-4} for different modulation formats is shown in Table 1. From this table, it is clear that the DST-LFDMA system and the DFT-LFDMA system provide the same PAPR performance whereas the PAPR of the DST-IFDMA system is higher than that of the DFT-IFDMA system by about 1.5 dB and 1 dB for the QPSK and 16QAM, respectively.

8 Conclusion

In this paper, we propose a new transceiver scheme based on the DST for future wireless communications, namely DST-SC-FDMA. The system model of the DST-SC-FDMA system has been derived and its performance has been studied and compared with the existing systems. Simulation results have been shown that the DST-SC-FDMA system provides superior BER performance than the DFT-SC-FDMA and the OFDMA systems. It is also found that the BER performance of the DST-SC-FDMA system is the same as that of the DCT-SC-FDMA system. Results have also been demonstrated that the PAPR performance of the DST-LFDMA system is the same as that of the DFT-LFDMA system and better than that of the DCT-LFDMA and the OFDMA systems.

9 References

[1] 3rd Generation Partnership Project (3GPP) Technical Specification Group Radio Access Network; Physical Layer Aspects for Evolved Universal Terrestrial Radio Access (UTRA) (Release 7). 3GPP TR 25.814, V7.1.0, September 2006

[2] Myung H.G., Goodman D.J.: 'Single-carrier FDMA a new air interface for long term evolution' (John Wiley & Sons, Ltd., 2008)

[3] Myung H.G., Lim J., Goodman D.J.: 'Single-carrier FDMA for uplink wireless transmission', *IEEE Veh. Technol. Mag.*, 2006, **1**, (3), pp. 30–38

[4] Al-kamali F.S., Dessouky M.I., Sallam B.M., Shawki F., Al-Hanafy W., Abd El-Samie F.E.: 'Joint low-complexity equalization and carrier frequency offsets compensation scheme for MIMO SC-FDMA systems', *IEEE Trans. Wirel. Commun.*, 2012, **11**, (3), pp. 869–873

[5] Al-kamali F.S., Dessouky M.I., Sallam B.M., Abd El-Samie F.E., Shawki F.: 'A new single-carrier FDMA system based on the discrete

cosine transform'. ICCES'9 Conf., Cairo, Egypt, 14–16 December 2009, pp. 555–560
[6] Al-kamali F.S., Dessouky M.I., Sallam B.M., Shawki F., Abd El-Samie F.E.: 'Equalization and CFOs compensation for the SC-FDMA system with different basis functions'. *Wirel. Pers. Commun.*, 2012, **67**, pp. 113–138
[7] http://en.wikipedia.org/wiki/Discrete_sine_transform
[8] Al-kamali F.S., Dessouky M.I., Sallam B.M., Abd El-Samie F.E., Shawki F.: 'Transceiver scheme for SC-FDMA Implementing the wavelet transform and the PAPR reduction methods', *IET Commun.*, 2010, **4**, (1), pp. 69–79
[9] 3rd Generation Partnership Project, 3GPP TS 25.101 – Technical Specification Group Radio Access Network; User Equipment (UE) Radio Transmission and Reception (FDD) (Release 7), Section B.2.2, September 2007